Multiple beam interference with near-grazing waves in dielectric wedges: polarization dependence

G. Rodríguez-Zurita, J. Vázquez-Castillo, and J. Pedraza-Contreras
Facultad de Ciencias Físico-Matemáticas, Benemérita Universidad Autónoma de Puebla, Apartado postal 948, Puebla 72000, Pue. Mexico.

Recibido el 18 de agosto de 2003; aceptado el 2 de febrero de 2004

Multiple beam interference of near-grazing waves has been recognized as responsible for bright interference patterns in dielectric wedges. Near-grazing waves are traveling waves having wave vectors forming an angle of nearly $\pi/2$ with the normal of a planar surface. When two such surfaces form a wedge with near-grazing waves within, two main features determine interference pattern formation. First, the values of the Fresnel reflection coefficients are close to unity for near-grazing waves. Second, the phase dependence as a function of the gap between surfaces is step-wise nearly constant for the same kind of waves. Both features have polarization dependence, so polarization dependence of interference patterns are also expected. Numerical results for s and p polarizations are presented under monochromatic and polychromatic illuminations. Experimental observations are also shown.

Keywords: Interference; polarization; dielectric interfaces.

La contribución de la interferencia de múltiples ondas casi-rasantes se ha reconocido como responsable de los brillantes patrones de interferencia que aparecen en cuñas dieléctricas. Por ondas casi-rasantes entendemos ondas viajeras cuyos vectores de propagación forman ángulos cercanos a $\pi/2$ respecto de las superficies dieléctricas planas. Cuando dos de estas superficies se acercan para formar una cuña conteniendo ondas casi-rasantes, aparecen dos características que determinan la formación de patrones de interferencia. Primero, los valores de los coeficientes de reflexión de Fresnel resultan cercanos a la unidad. Segundo, la dependencia de la fase como función de la separación entre las interfaces sigue un comportamiento constante por tramos. Ambas características dependen de la polarización de las ondas interferentes, de modo que es de esperarse una dependencia en la polarización por parte de los patrones de interferencia. Se presentan resultados numéricos para las polarizaciones sy p bajo iluminaciones tanto monocromática como policromática. Se muestran también observaciones experimentales.

Descriptores: Interferencia; polarización; interfaces dieléctricas

PACS: 42.25.H; 07.60.L; 78.66; 82.80.C

1. Introduction

A bright interference pattern can be observed when two plane dielectric surfaces are brought together so as to form a wedge [1]. Fringes can be seen under rather ordinary wedge angles (of the order of some *mdeg*). Although at first sight this effect can be considered as a two beam Heidinger-type interference effect, a closer inspection under monochromatic illumination reveals certain finesse in the fringes, which is typical of multiple beam interference patterns. Moreover, the fact that illuminating wedges with a polychromatic source also produces visible interference patterns suggests that the optical path lengths of the interfering waves somehow do not change too much whenever this effect is detectable.

For the monochromatic case, the above considerations lead to a multiple beam Fizeau interference process as described in [2]. But observed conditions for pattern appearance includes propagating angles of the involved waves with values close to $\pi/2$ with respect to the surface's normals (near-grazing waves) instead to be close to 0 rads [1]. Besides, the existence of polychromatic patterns dictates that the interfering waves have to be near-grazing ones. The reason for this is the particular phase behavior of the electric field of the superposition of this kind of waves as function of gaps, as shown in the analysis done in connection with studies about evanescent contributions to total fields arising from multiple reflections in dielectric slabs [3]. Such behavior shows piecewise constant regions not only for evanescent waves but also for near-grazing propagating waves. This fact gives as a the main difference with the well-known case of having propagating angles close to 0 rads [4], where polychromatic interference patterns are not so directly observed.

These considerations have been reported previously in some detail for the monochromatic case as well as the polychromatic case [5]. However, the scope was limited to the s or perpendicular polarization of the interfering light beams. Because the conditions of appearance for the interference patterns under discussion are polarization dependent, a corresponding dependence of patterns on light beams polarization are to be expected. The purpose of this work is to inspect the main consequences of polarization on the interference patterns formed by multi-beam Fizeau interference with near-grazing waves. Monochromatic and polychromatic cases are taken into account. Numerical results are presented and experimental observations are also shown.

2. Multiple interference and polarization

2.1. Near-grazing waves generation

Multiple near-grazing waves are generated with rectangular prisms as depicted in Fig. 1. In Fig. 1a, a ray impinges on

a cathetus face of a rectangular prism in point A at the angle $\theta \neq 0$. It is then refracted at the angle θ', and goes to the hypotenuse at point B, where it suffers total internal reflection at an angleθ_1' larger than the prism critical angle θc. At this point, generation of evanescent waves occurs in the surrounding medium. After this reflection, the ray travels to point C at angle θ' over the other cathetus face, where a partial reflection occurs this time. The reflected ray continues to point D, where it is incident at angle $\theta_2'$to be later transmitted at angle $\theta_2 \approx \pi/2$ whenever θ remains within a certain range of values. It can be shown that

$$\theta_1' = \pi/4 + \theta', \tag{1}$$

and

$$\theta_2' = \pi/4 - \theta'. \tag{2}$$

The angles θ and θ_2 can be determined by Snell's law. In Fig. 1b, the ray impinges opposite to the of on the prism's face at point A but in the other side of the surface's normal as in case of Fig. 1a. Generation of near-grazing waves occurs at point D directly, and Eq.2 remains valid. Both cases of Fig.1 give two variants to generate multiple beam near-grazing waves. This is shown correspondingly in Fig.2, where waves are generated between the hypotenuses of two rectangular prisms. In such a pair of prisms, θ is the angle of incidence with respect to the entrance face of the first prism and α denotes the angle of the wedge.

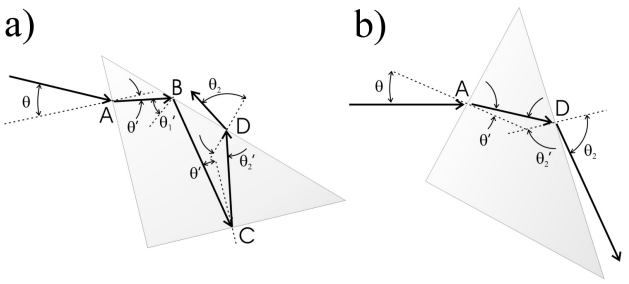

FIGURE 1. A simple ray tracing to illustrate how generation of near-grazing waves can be carried out using rectangular prisms in two situations.

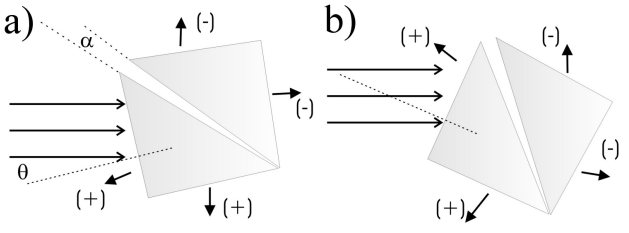

FIGURE 2. An air wedge formed between two prisms. A light beam is incident at angle θ as shown in the two variants. According to experimental observations, the symbols (+) and (-) denote observed interference patterns of opposite contrasts.

2.2. Polarization dependence of the phase of total field for near-grazing waves ($\alpha = 0$)

Following Ref. 3, the phase of total field due to the superposition of multiple beams within a dielectric slab's gap ($\alpha = 0$) was calculated for several wavelengths λ and a glass type (BK7). Refractive indices for each wavelength were determined by the dispersion formula

$$n^2 = A_0 + A_1\lambda^2 + A_2\lambda^{-2} + A_3\lambda^{-4} + A_4\lambda^{-6} + A_5\lambda^{-8}, \tag{3}$$

and introducing the proper coefficients as given by Ref. 6 (wavelength in μ m). Results are calculated and shown in the Fig. 3. In general, the phase shift as a function of gap a ($\alpha = 0$) for different anglesθ_2' (which departs from critical angle θc by some *mrad*) show a stepwise constant behavior for both polarizations s and p. Wavelengths 632.8 nm, 542.5 nm, and 488 nm were used together with their respective refractive indices for the same BK7 type glass. Plot for case s and θc-1 *mrad* runs very close to the horizontal axis at the used scale. The phase of polarization s remains constant in wider ranges that the phase of polarization p within the range of values considered. There is relatively little change for the different wavelengths. These are the features of near-grazing waves which conspire to interference fringe formation with white light.

2.3. Multiple beam superposition of near-grazing waves

In order to calculate the multiple beam interference pattern due to a wedge for different linear polarization illumination, the following well-known phase shift relation for δ_p [2] can be first employed (see Fig. 4),

$$\delta_p = (4\pi/\lambda)\, n' \cdot \rho \left\{\sin\left[(p-1)\,\alpha\right]\cos[\upsilon_p']\right\} \left\{\cos\left[(p-1)\,\alpha\right] - \tan[\upsilon_p']\sin\left[(p-1)\,\alpha\right]\right\}, \tag{4}$$

where n and n' denote the refractive indexes of the wedge and of both prisms respectively, ρ for the position on the second side of the wedge, $\upsilon_p' = \upsilon' + 2(p-1)\alpha$ for the angle of the wave within the wedge, and p indicating the number of reflections taken to be 5 according to our experimental observations. Also, $\upsilon' = \upsilon_1' = \theta_2 + \alpha$. Thus, the total field $A^{(t)}$on the second surface would be

$$A^{(t)} = A^{(i)} t(\theta_2') \sum_{p=1}^{N} \left\{ A^{(p)} t' \left[\upsilon' + 2\,(p-1)\,\alpha\right] \times \prod_{q=0}^{2(p-1)} r'\left(\upsilon' + q\alpha\right) \right\} \cos\delta_p, \tag{5}$$

where $r'(\upsilon)$ and $t'(\upsilon)$ are the Fresnel reflection and transmission coefficients at the angle υ from index n to n', $A^{(i)}$ denotes the amplitude of incidence and $A^{(p)}$ is equal to unity for s polarization, while it becomes equal to $\exp\{i\upsilon_p\}$ for p

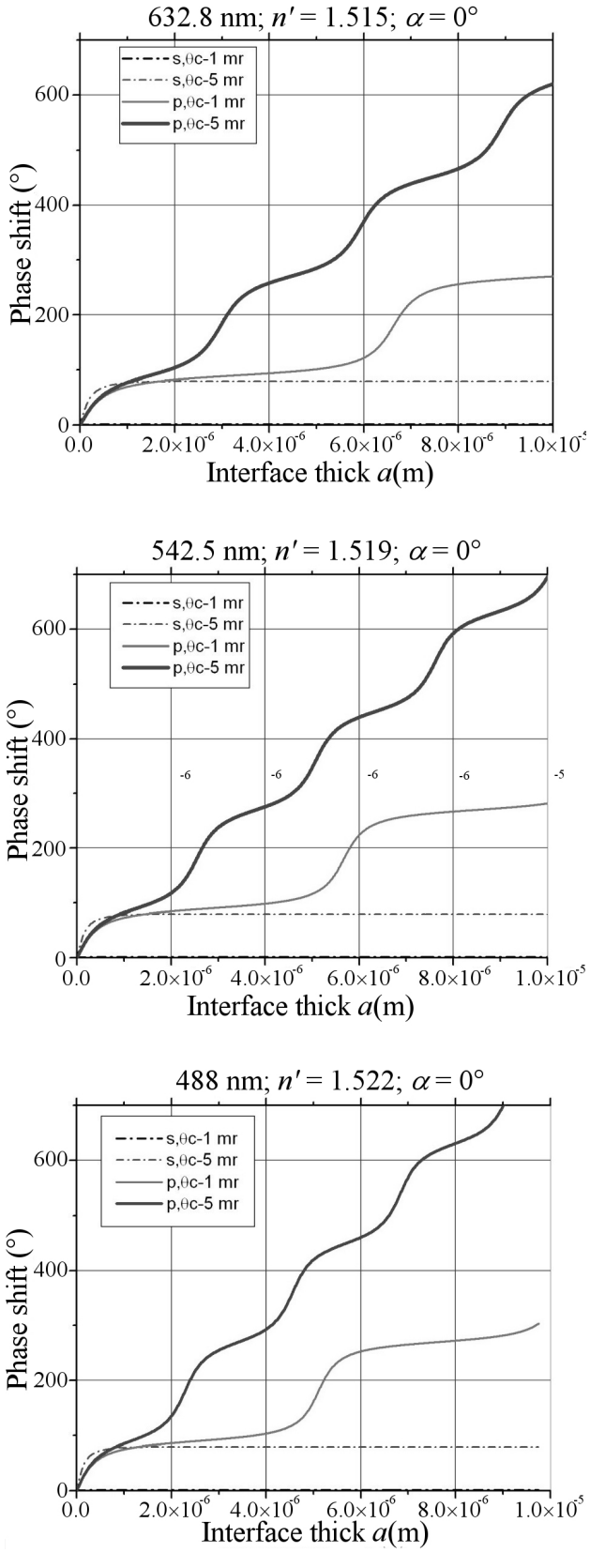

FIGURE 3. Phase shift as a function of gap a ($\alpha = 0$) for different departures from critical angle θc and for both polarizations s and p (632.8 nm, 542.5 nm and 488 nm).

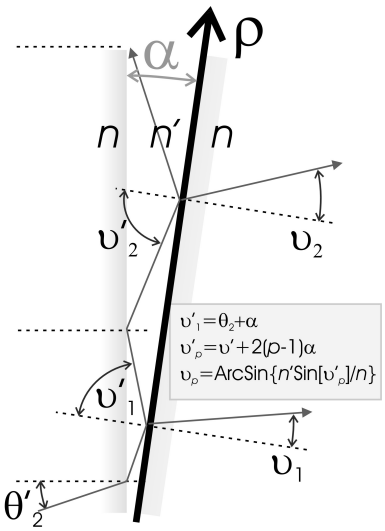

FIGURE 4. Wedge parameters. $\upsilon_1 = \pi/2 - \theta_2$ and $\mathbf{p}$ runs from $\mathbf{p} = 1$.

polarization. $t(\theta_2')$ denotes the transmission Fresnel coefficient from index n to index n'. This describes the crossing of the waves from the first prism into the wedge. Total irradiance is calculated in arbitrary units as $I^{(t)} = A^{(i)}A^{(i)*}$.

To take glass dispersion into account, the dispersion formula, Eq. 3, was used to calculate refractive indexes using appropriate coefficient values as described above. Chromaticity diagrams are obtained following standard procedures [7] and with the help of $I^{(t)}$.

3. Numerical results: $s-$ and $p-$ polarization

3.1. Multiple beam versus two-beam (α, θ constants)

Figure 5 compares the numerical results of multiple beam interference patterns (both polarizations) with two-beam interference patterns (dashed line) at the same wedge angle $\alpha = 0.02°$ and incidence at $\theta = 7°$ for BK7 glass type only. Interference patterns of (-) contrast are solely presented. This kind of patterns denotes bright narrow fringes and wider dark fringes, as opposite to the complementary contrast denoted by (+). The figure shows the monochromatic case in the left and, at the right, the polychromatic case on shows.

3.1.1. Monochromatic case

Fringe density is different between multiple beam interference pattern and two-beam interference pattern (632.8 nm was used). As it is also well known for the case of multiple beam interference in dielectric wedges at normal incidence, there is no symmetry around each maxima [2,4]. Fringe contrast is different for each polarization. More structure appears in the interference pattern for the $s-$ polarization case than for the $p-$ polarization case. Maxima from multiple beam interference are located at the same place, at least approximately.

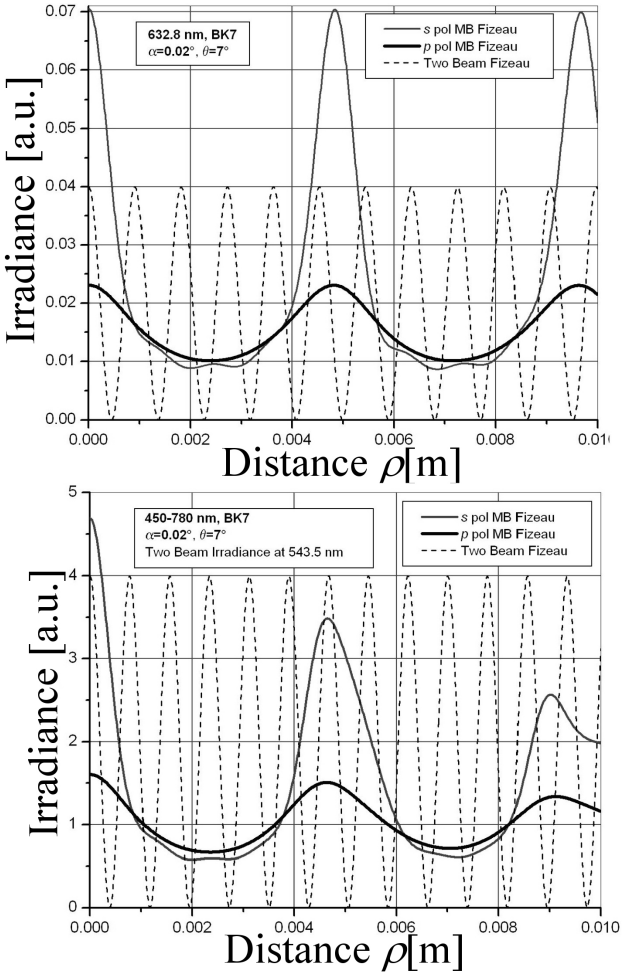

FIGURE 5. Multiple-beam interference patterns with contrast (-) at $\theta = 7^\circ$ or $s-$ and $p-$ polarizations as compared with two-beam interference patterns (dashed line) for the same value $\alpha = 0.02^\circ$. BK7 glass type. Monochromatic case ($\lambda = 632.8$ nm) on the left. Polychromatic case ($\Delta\lambda\{450; 780\}$ nm and $\lambda = 543.5$ nm for two beams) on the right.

3.1.2. Polychromatic case

Although a polychromatic beam with a wide bandwidth $\Delta\lambda$comprising from 450 nm to 780 nm (equal weight) was considered, interference patterns do occur in agreement with experimental observations. They are compared with a two-beam interference pattern calculated at 543.5 nm. Due to dispersion, appearance of propagating waves at a given λdepends on the angle of incidence θ. This fact defines the limits of the bandwidth whose components contribute to the pattern. The width of each of the maxima is wider than the monochromatic case, especially those of higher orders. Chromatic fringes, of course, are not described in this kind of plots because they are irradiance plots only. Fringe contrast is again different for each polarization.

3.2. Monochromatic multiple beam interference patterns for several values of α and θ

Monochromatic multiple beam interference patterns were calculated for each polarization of the illuminating beam for several wedge angles α and incidence angles θ, and then plotted in Fig. 6. Values of these angles are indicated at the margins of each plot. As a way to visualize polarization changes, the quotient of amplitudes of $s-$ and $p-$ polarizations were also plotted (thick line). These plots can then be thought of as the polarization of the corresponding interference pattern as a function of the position ρ when the incident illuminating beam has linear polarization forming 45° with respect to the incidence plane.

Fringe contrast is different for each polarization case as before (Fig. 5). But for low values of θ, the height of maxima is greater for $p-$ polarization than for $s-$ polarization. This tendency reverses for larger values of θ. $s-$ polarization patterns also show more structure than the $p-$ polarization ones. The variation of the polarization angle has more oscillations for larger values of θ.

3.3. Polychromatic multiple beam interference patterns for several values of α and θ

Polychromatic multiple beam interference patterns were calculated for each polarization of the illuminating beam for several wedge angles α and incidence angles θ, and then plotted in Figs. 7 and 8. $\alpha = 0.02^\circ$ in Fig. 7 with $\theta = 7.5^\circ$ in Fig. 7a and $\theta = 8^\circ$ in Fig. 7b. The larger the value of θ, the wider the fringes of higher orders. In Fig.8, the values of these angles are indicated at the margins of each plot. Patterns associated with $s-$ polarization have more secondary maxima than $p-$ polarization ones and the asymmetry about each principal maximum is more clearly seen for that case. Fringe contrast is different for each polarization case as before (Figs.5 and 6). Oscillations of patterns tend to disappear due to the contribution of different wavelengths, especially for $p-$ polarization.

Chromaticity diagrams can be calculated from intensity values assuming a given illuminant spectral distribution. As a preliminary result, Fig. 9 shows two CIE-1931 chromaticity diagrams for each polarization, and for an ideal illuminant with unity radiance for each one of its components. Values of used angles are $\alpha = 0.06^\circ$ and $\theta = 6.3^\circ$. In the case of $s-$ polarization (Fig. 9a), chromaticity coordinates spread themselves over the chromaticity diagram more to the greens than the ones of $p-$ polarization (Fig. 9b), which values concentrate along a line between blues and yellows. A more detailed inspection (as location of chromatic coordinates belonging to maxima) has to be done to extract conclusion related to chromatic variations, but changes of color as function of dispersion or polarization could be used to characterize glass types, for example.

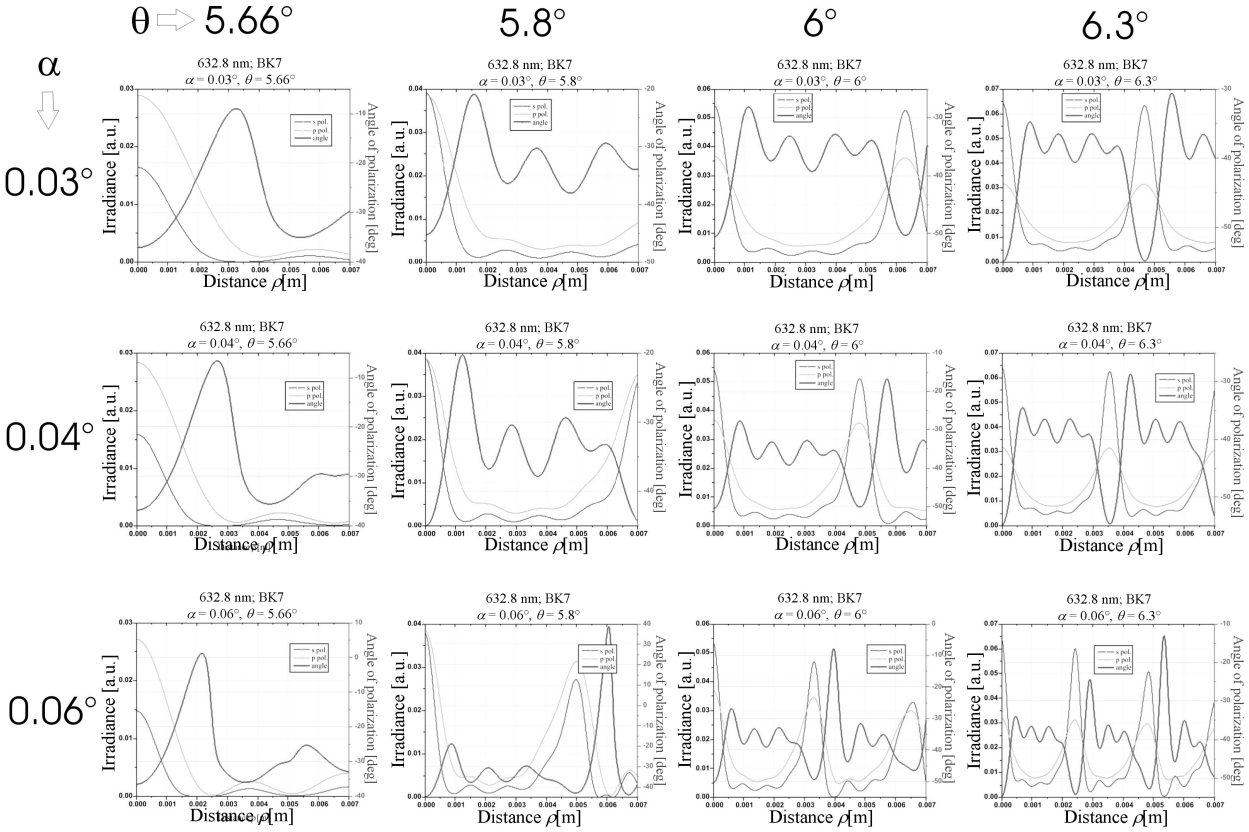

FIGURE 6. Some monochromatic patterns for several values of θ (in a row, above) and α (in a column, left). $\lambda = 632.8$ nm and BK7 glass type. Polarization angle in thick line.

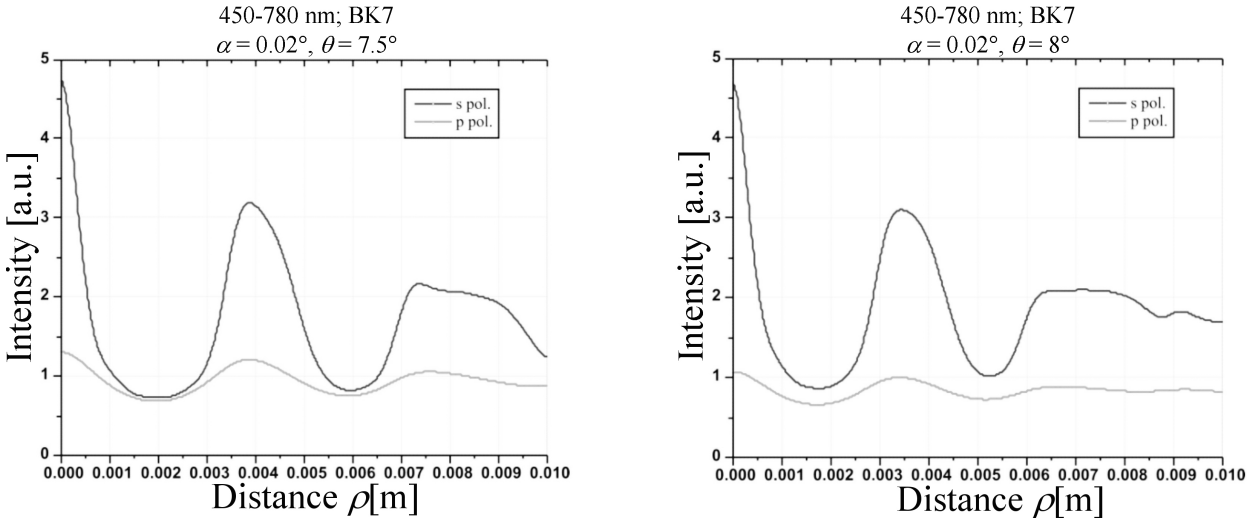

FIGURE 7. Polychromatic patterns for $\alpha = 0.02°$ and two values of θ: a) 7.5° and b) 8°. $\Delta\lambda$ runs from 450 nm to 780 nm. BK7 glass type. $s-$ polarization patterns result above the p-polarization patterns in both cases.

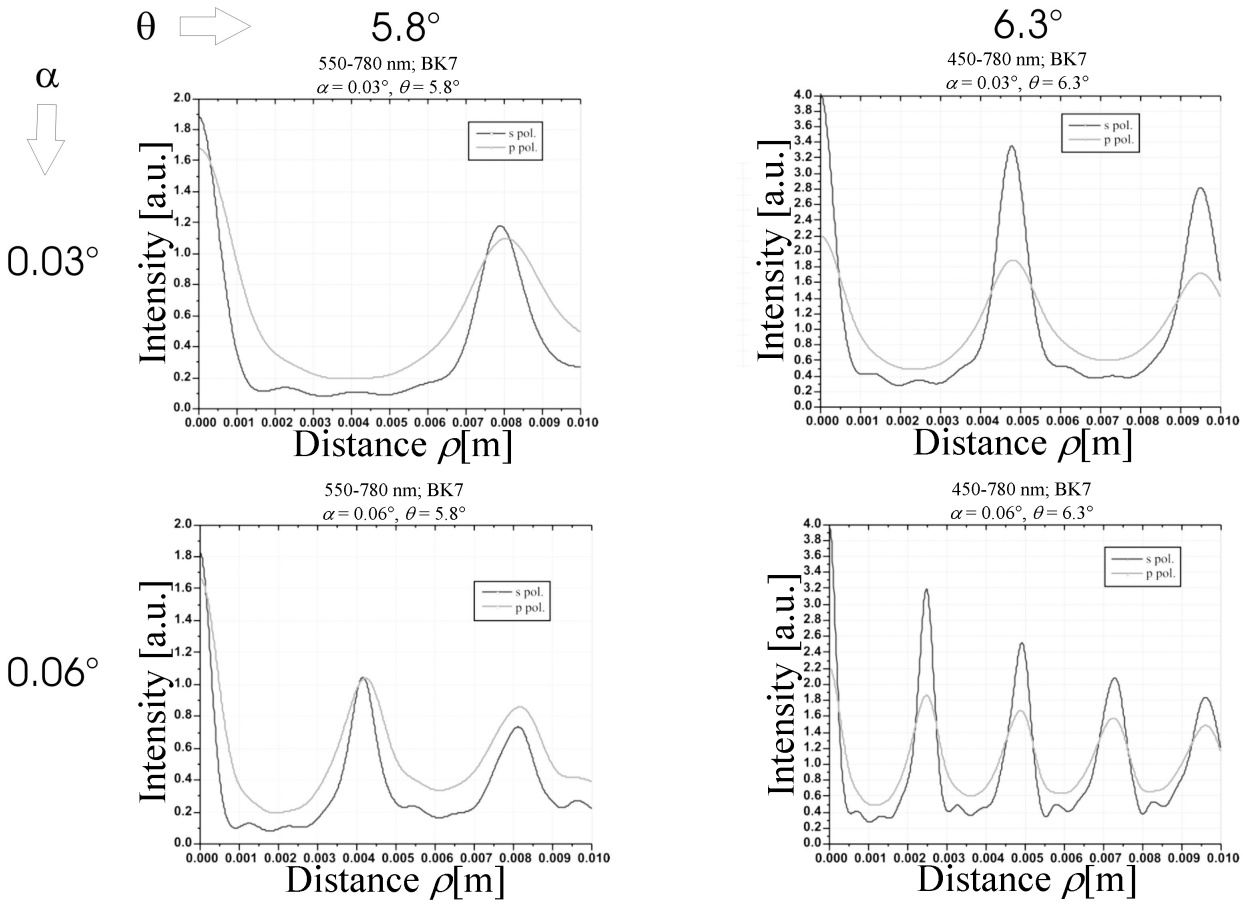

FIGURE 8. Some polychromatic patterns for several values of θ (in a row, above) and α (along a column, left). $\Delta\lambda$ runs from 550 nm to 780 nm for $\theta = 5.8^\circ$ and from 450 nm to 780 nm for $\theta = 6.3^\circ$. BK7 glass type. $s-$ polarization patterns result above the p-polarization patterns except in case $\theta = 5.8^\circ$ and $\alpha = 0.06^\circ$.

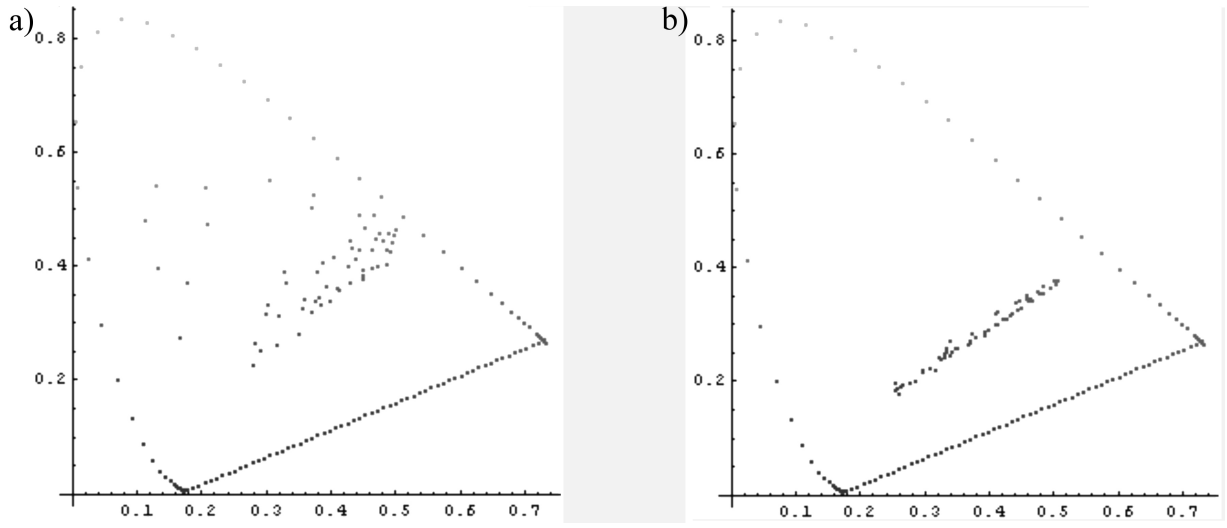

FIGURE 9. CIE 1931 chromaticity diagrams for $s-$ polarization (a) and $p-$ polarization (b).

4. Experimental set-up

The experimental set-up for inspection of these properties is shown in Fig. 10. Collimated illumination with adjustable linear polarization coming from the left at angle θ generates near-grazing multiple beams in the wedge between the prism and the cube beamsplitter. Angle θ can be varied because the entrance prism, the beamsplitter and the illuminating system

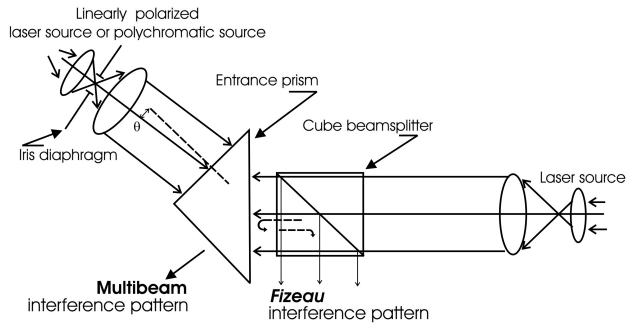

FIGURE 10. Experimental set-up.

from the right form a whole system all together being attached on a common rotating bench. Thus, a multiple beam interference pattern can be observed as θ changes. At the same time, the collimated laser source from the right forms a two-beam Fizeau interferometer working at normal incidence without dependence on θ. This serves for measuring the wedge angle α by standard procedures. A polarized (vertical) stabilized He-Ne laser beam emitting red light was used for multiple beam pattern generation. To control the polarization of the illuminating beam, a quarter-wave plate, at 45° to achieve nearly circular polarization, was employed. The plate was followed by a polarizing filter to attain vertical or horizontal linear polarizations. To illuminate the Fizeau interferometer, another vertically linear polarizated He-Ne laser emitting green light was used. Comparison of patterns with the main theoretical conclusions outlined can be carried out this way. In the following photographs, note the correspondence in shape between multiple- and two-beam interference patterns.

4.1. Monochromatic illumination

4.1.1. $p-$ and $s-$ polarization of the illuminating beam

Figure 11 shows experimental interference patterns registered for an angle α whose value is estimated as 0.01° (see the Fizeau pattern at Fig. 11c). The polarizer to control illuminating beam was adjusted for either $s-$ polarization or $p-$ polarization. Photographs were taken with no analyzer. As deduced from the exposure values, this is a case of comparable (or even greater) irradiance for the p case than for the s case. Figure 12 shows differences in the structure between the two polarizations. A bright fringe appears close to a dark one of the first order only in the $s-$ polarization. Figure 13 shows a difference in width of patterns taken at larger θ values. Irradiance for $p-$ polarization is lower than for $s-$ polarization. Fringe width is clearly narrower for $s-$ polarization. These observations qualitatively agree with the calculations of Fig. 6 in respect to irradiance, pattern structure and fringe widths.

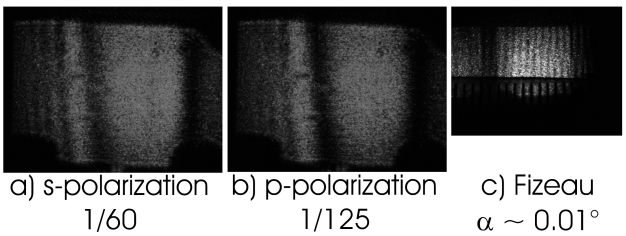

FIGURE 11. Experimental monochromatic multiple beam interference patterns for low value of θ. $s-$ polarization (thin line) and $p-$ polarization (thick line), both taken with f/3.6 aperture at $\lambda = 632.8$ nm. Exposure times 1/60 (s) and 1/125 (p). c) two-beam Fizeau interference pattern (dashed line) at $\lambda = 543.5$ nm.

4.1.2. 45° linear polarization of the illuminating beam

Patterns registered by employing an analyzer in front of the camera objective are presented in Fig. 14. Incident linear polarization was adjusted to 45° approximately. Transmission angle of the analyzer relative to the horizontal is indicated in each picture, together with the respective exposure times. All pictures were taken at an aperture of f/3.6. Changes in the structure of patterns are observed. Dark fringes with wider width appear above and below, in particular, around the value of 125° for the analyzer transmission axis. A bright, narrow fringe remains close to the one almost in diagonal position.

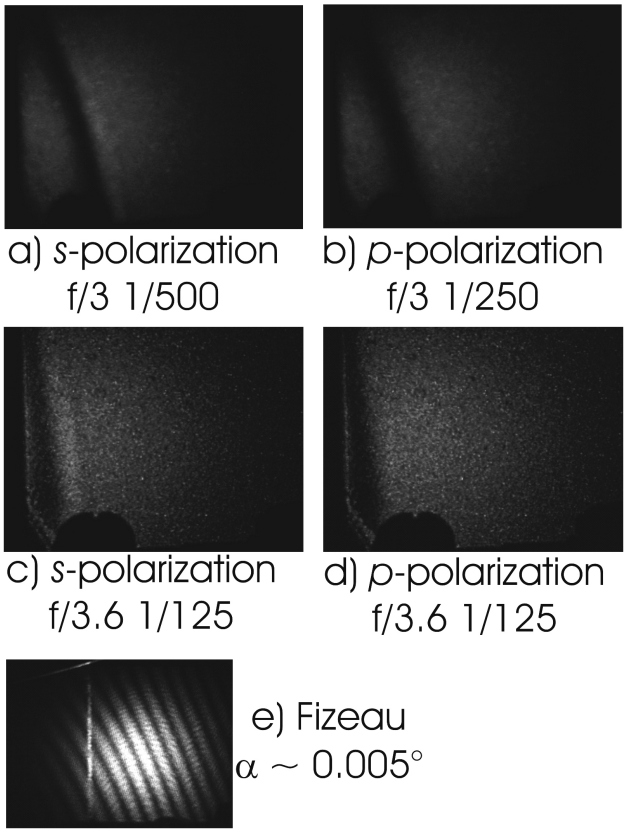

FIGURE 12. Experimental monochromatic multiple beam interference patterns for other values of θ: a) and b) under the same θ value, and c) and d) under a second value. a) and c) $s-$ polarization and b) and d) $p-$ polarization. Apertures and exposure times as indicated. e) Corresponding two-beam Fizeau interference pattern.

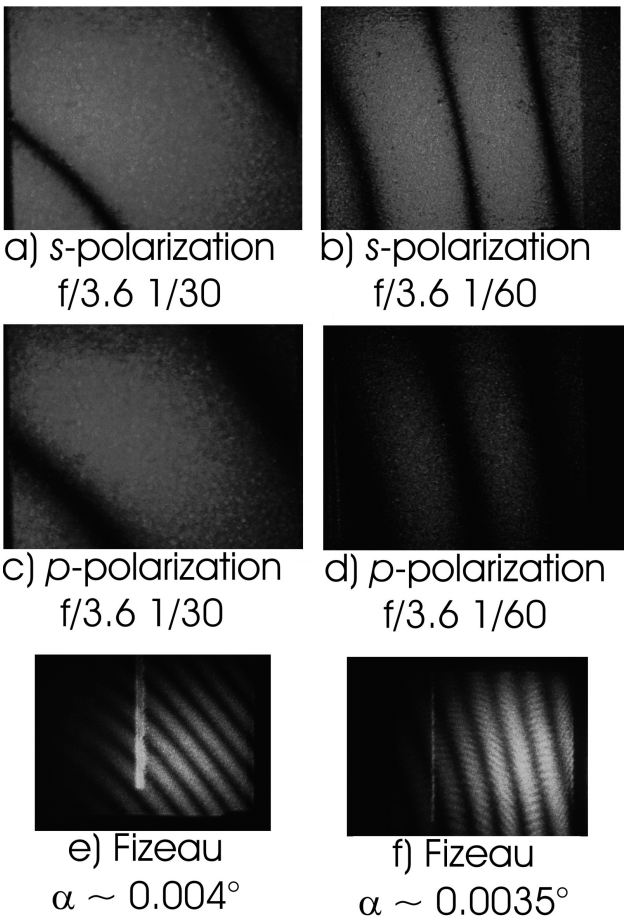

FIGURE 13. Experimental monochromatic interference patterns for larger values of θ: (a) and (b) under $s-$ polarization, while (c) and (d) under $p-$ polarization. a), c) and e) the same value of θ and α. b) d) and f) with the same value of θ and α. Apertures and exposure times as indicated.

This fringe seems to result from the wider fringe which ap pears at 110°, as if it came from a "splitting" process. This effect can be related to the numerical results plotted in Fig. 6, because they state that the polarization does not remain constant over the interference pattern.

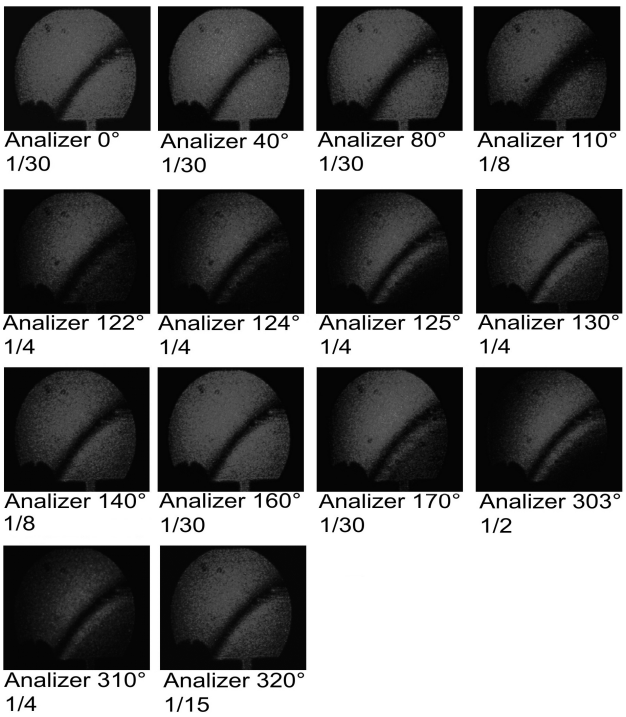

FIGURE 14. Experimental monochromatic multiple beam interference patterns for linear polarization of the illuminating beam at 45°. Observations were made using an analyzer in front of the camera. The linear polarization of the analyzer with respect to the horizontal is indicated in each picture. Aperture for all photographs: f/3.6. Exposures times as indicated.

4.2. Polychromatic illumination

As for observations under polychromatic illumination, drastic changes in contrast of the fringes were observed for each polarization of the incident light. An example is shown in Fig. 15. This observation agrees with Figs. 7 and 8. However, chromatic changes other than saturation modifications are not very noticeable.

FIGURE 15. Experimental polychromatic multiple beam interference patterns.

5. Final comments

Some influences from the polarization of light involved in interference patterns generated by near-grazing waves within dielectric wedges were investigated. Basic considerations allow the finding of the principal properties of patterns formed by monochromatic as well as polychromatic illumination. As a general conclusion, it is stated that the polarization of the illuminating beams is an issue whose influence, somewhat noticeable in experiments, has to be taken into account when trying to extract information of dielectric properties by using multi-beam interferometric effects. The changes of pattern structures depending on the polarization are very important to consider when reliable results are to be found.

Applications of the case of dielectric wedges can appear while characterizing dispersion properties of bulk samples from optical glasses because the interference patterns varies in their chromatic coordinates [5]. Moreover, because variable gaps are formed during material fractures, the interferometric effects than can be generated could give information of some utility on that respect. Generalization to materials other than isotropic linear dielectric ones (as metals, anisotropic dielectrics, or non-linear materials) can be worthy of some further inspection along the prescribed lines just presented.

Acknowledgements

Partial support from CONACyT (41704) is appreciated. Some results were presented at the ICO Topical Meeting on Polarization Optics 2003.

1. J. Pedraza-Contreras, G. Rodriguez-Zurita, A. Cornejo-Rodriguez, and O. Cardona-Núñez, *Rev. Mex. Fís.* **40** (1994) 7.
2. M. Born and E. Wolf, *Principles of Optics*, (Fifth edition, Pergamon Press, Oxford 1975), p.351.
3. C.K. Carniglia and L. Mandel, *JOSA* **61** (1971) 1035.
4. C. Roychoudhuri, *Multiple-beam interferometers*, C.6 in *Optical Shop Testing*, (ed. D. Malacara, Wiley Series in Pure and Applied Optics, New York 1978).
5. G. Rodriguez-Zurita, J. Pedraza-Contreras, R. Pastrana-Sanchez, A. Cornejo-Rodriguez, and J.F. Vazquez-Castillo, *Rev. Mex. Fís.* **44** (1998) 147.
6. Optisches Glas, Katalog 011S, VEB JENAer Glaswerk Schott & GEN., Jena.
7. G. Wyszecki and W. S. Stiles, *Color Science. Concepts and methods, quantitative data and formulae*, (2nd ed., Wiley, New York 1982).